

# A Novel Technology to Develop a Nickel-Enriched Layer on Slab Surface by Utilizing NiO-Containing Synthetic Powder



TAE-IN CHUNG, JUNG-WOOK CHO, and YOUN-BAE KANG

Cu, as one of the typical tramp elements, is known to cause hot shortness during reheating of slabs followed by hot rolling of sheet products. In order to prevent such harmful aspects, a new idea is proposed by using synthetic powders containing NiO in the mold flux during continuous casting of the slab. During the casting, NiO is reduced and absorbed on initial solidified steel shell, and a Ni-rich layer is developed near the surface region of the slab. According to the proposed idea, it is expected that both the Cu solubility and the melting temperature of Cu-segregated region would increase considerably by virtue of Ni-rich layer, which is believed to play an important role to prevent the Cu hot shortness. A series of laboratory-scale experiments were carried out in order to confirm the reduction and the absorption of Ni into the steel matrix. It was observed by SEM-EDS and FE-EPMA that a Ni-enriched layer, as thick as a few hundred  $\mu\text{m}$ , formed near the surface of the slab. Also, a number of laboratory-scale heat treatment tests under oxidizing atmosphere showed that the samples with the Ni-enriched layer had a decreased Cu enrichment at the interface between scale and steel, compared to a case without Ni-rich layer. A pilot-plant-scale steel slab (medium carbon steel containing 0.3 wt pct Cu) was obtained in a continuous casting process with the NiO-containing mold flux, and a Ni-enriched layer was also observed. It was concluded that the use of NiO in the mold flux is a promising new approach for suppressing the hot shortness of Cu-containing steel, without an expensive addition of Ni to the whole steel matrix.

DOI: 10.1007/s11663-015-0459-y

© The Minerals, Metals & Materials Society and ASM International 2015

## I. INTRODUCTION

IN these days, most of steelmakers in the world are trying to reduce CO<sub>2</sub> emission during ironmaking and steelmaking processes. As one of the activities to reduce the CO<sub>2</sub> emission, they have been trying to use ferrous scrap as much as possible during steelmaking process in converter. The use of hot metal containing high content of C is reduced significantly by the so-called “low hot metal process”. This process also has an additional merit in such a way that, depending on the market price of the scrap and the hot metal, it can flexibly adjust input amounts of the scrap and the hot metal in order to optimize production cost. However, using the scrap inevitably introduces tramp elements such as Cu and Sn into steel products. As Cu has less affinity with O than Fe has, it is very difficult to remove the Cu by O blowing in the basic oxygen-blowing process.<sup>[1]</sup> Furthermore, the remained Cu is not oxidized during reheating process, due to a selective oxidation of Fe on slab surface by the same reason. This results in Cu to be enriched at the

interface between oxidized scale and steel matrix. When the slab is reheated at temperature over 1373 K (1100 °C), the enriched Cu forms at the steel/scale interface, and easily infiltrates into the austenite grain boundary, and induces the inter-granular cracking during hot rolling. This is known as the surface hot shortness by Cu enrichment.<sup>[2,3]</sup>

In order to minimize such undesired aspects of scrap recycling, there have been two major research directions. One is a direct removal of Cu from scrap or liquid steel. This includes low melting point bath,<sup>[4]</sup> chlorination,<sup>[5–8]</sup> sulfide flux refining,<sup>[9,10]</sup> and vacuum distillation.<sup>[11–15]</sup> However, these have not been yet adapted in industries due to their insufficient Cu removal efficiency, high operation cost, and longer process time. The other direction is to suppress the Cu enrichment during the reheating process. While making Cu to be left in the steel, it aims to suppress harmfulness of the Cu by treating the steel in various ways: Ni/Si alloying,<sup>[16–19]</sup> reheating Cu-containing slab at higher temperature than fayalite melting point,<sup>[3,16]</sup> and mechanical shot peening.<sup>[20]</sup> Among these ideas, the Ni alloying has been widely used in several industries. Alloying Ni increases the solubility of Cu in  $\gamma$  matrix. This yields less precipitation of Cu-enriched phase during the reheating. Although not actively used in the industries, increasing the reheating temperature over 1473 K (1200 °C) results in the formation of molten fayalite phase which absorbs the Cu-enriched phase at this temperature. This reduces

TAE-IN CHUNG, Senior Researcher, is with the Technical Research Laboratories, POSCO Ltd., Republic of Korea. JUNG-WOOK CHO, Research Associate Professor, and YOUN-BAE KANG, Associate Professor, are with the Graduate Institute of Ferrous Technology, Pohang University of Science and Technology, Republic of Korea. Contact e-mail: ybkang@postech.ac.kr

Manuscript submitted May 4, 2015.

Article published online September 14, 2015.

the harmfulness of the Cu hot shortness. However, despite of their effective role, these methods have not been successfully commercialized because the addition of Ni or increasing the reheating temperature leads to high production cost and poor productivity. Recently, a cost-effective idea was newly suggested: mechanical shot peening on steel surface can increase the surface roughness and reduce the copper enrichment by separating Cu-enriched phase at the slab surface.<sup>[20]</sup> However, this idea was also found to have a limitation that the roughness on surface of the slab disappears within only 60 minutes from the starting of oxidation by the reheating. All these observations require further cost-effective technology to suppress the Cu enrichment as long as the ferrous scrap is used without pre-treatment for the Cu removal.

The present investigation focuses on how Ni alloying could be effectively done with respect to the suppression of the Cu enrichment during reheating process. In previous practices, Ni should have been available up to 2 times of Cu content over whole steel slab, although the Cu enrichment responsible for the Cu hot shortness occurs only near the surface of the steel slab.<sup>[17]</sup> This results in a high production cost, due to expensive use of Ni. In contrast, in the present study, a cost-saving and more effective idea for the Ni alloy is suggested. A conceptual method is shown in Figure 1. It is attempted that a Ni-enriched layer is developed only near the surface of steel slab, by a reaction between NiO-containing mold flux and steel in a casting mold during continuous casting process. The NiO may be easily reduced by alloying elements such as Mn, Si, and even Fe during the continuous casting, or C powder in the mold powder. The reduced Ni diffuses into the steel slab or enriches on the surface of the slab at initial solidifying temperature, although diffusion of Ni in the slab is slow. In order to evaluate feasibility of this concept, two investigations were carried out in the present study. First,

in order to confirm the reduction of NiO and subsequent diffusion of Ni in the steel matrix, a series of high-temperature diffusion couple experiments were conducted using a medium C steel and a number of synthetic mold powders. Second, the Ni-doped steel was examined for its susceptibility to the Cu enrichment behavior through an oxidation test. Based on these experimental results, finally, a process-simulating trial was conducted using a pilot-scale continuous caster, installed at Technical Research Laboratories, POSCO Ltd, Pohang.

## II. EXPERIMENTS

In the present study, a lab-scale experiment and a pilot-plant-scale experiment were carried out, respectively. The former was intended to confirm the idea proposed in the present study: NiO reduction–Ni diffusion–suppression of Cu enrichment near steel surface. The latter was carried out in order to realize this idea in a continuous casting condition.

### A. Lab-Scale Experiment: Reduction and Diffusion

A steel sample containing 0.4 wt pct Cu was prepared from a commercial continuous casting steel slab. The steel sample was homogenized in an electrical resistance furnace for 4 hours under Ar atmosphere, and was machined into a shape of cylinder (diameter: 30 mm, height: 15 mm) whose center was additionally machined to have a hole (diameter: 5 mm, height: 8 mm). A synthetic mold powder containing NiO as much as 2 g was put in the hole, as shown in Figure 2. The synthetic mold powder was prepared by mixing with a commercial mold powder for a continuous casting and a reagent grade of NiO powder (99.9 wt pct, Sigma-Aldrich Co.). Chemical compositions of the steel sample and the mold powder were analyzed by C/S analyzer (CS844, LECO), ICP-AES (Thermo Scientific ICAP 6500), and X-ray fluorescence analyzer (S4 Prioneer, Bruker Axs GmbH) as shown in Table I.

Figure 2(a) shows a thermal history of high-temperature reaction in order to investigate the NiO reduction in the synthetic mold powder, followed by Ni diffusion into the steel surface. The reactions were carried out in a vertical electric resistance furnace at 1673 K, 1713 K, and 1753 K (1400 °C, 1440 °C, and 1480 °C) for 30, 60, and 120 minutes, respectively. The atmosphere was controlled by dry Ar gas which was preliminarily purified by passing through a Mg chip heated at 723 K (450 °C). At each target temperature, the sample assembly (steel cylinder charged with the powder) was placed at the hot zone of furnace. As the melting temperature of the mold flux is 1443 K (1170 °C), the powder melted rapidly as the assembly was located at the hot zone. After holding for a predetermined time, the assembly was quickly quenched into water.

### B. Lab-Scale Experiment: Oxidation

Figure 2(b) shows another thermal history of high-temperature reaction in order to investigate

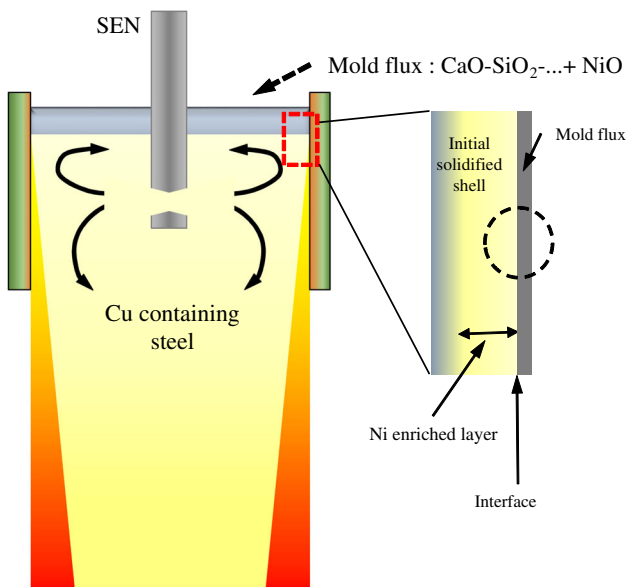


Fig. 1—Schematic drawing of the proposed idea in the present study.

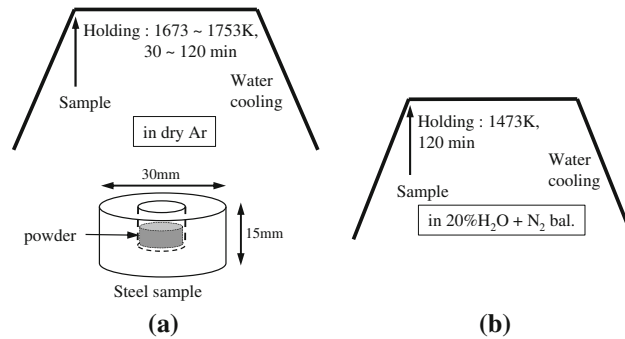


Fig. 2—Experimental conditions of high-temperature reaction and oxidation. (a) High-temperature reaction between NiO-containing mold powder and steel, and (b) high-temperature oxidation of Ni-coated steel under moisture gas condition.

**Table I. Chemical Composition of Steel and Synthetic Mold Power (in Weight Percent)**

| C                    | Si                             | Mn                             | Cu           | Ni*        |                   |                         |
|----------------------|--------------------------------|--------------------------------|--------------|------------|-------------------|-------------------------|
| 0.08 to 0.09         | 0.30 to 0.40                   | 1.50 to 1.60                   | 0.30 to 0.40 | 0.022      |                   |                         |
| CaO/SiO <sub>2</sub> | Al <sub>2</sub> O <sub>3</sub> | Fe <sub>2</sub> O <sub>3</sub> | F            | NiO        | Na <sub>2</sub> O | T <sub>m</sub> [K (°C)] |
| 1.1 to 1.2           | 5.0 to 6.0                     | 0.37                           | 6 to 7       | 4.0 to 5.0 | 4.0 to 5.0        | 1443 (1170)             |

\* impurity.

oxidation behavior of steel which had been reacted with the NiO-containing mold flux. The sample was obtained by the previous experiments described in Section II-A. The interface of the steel sample to the mold flux was polished in order to remove the reacted powder and to have a bare steel surface. The sample was held in the vertical electrical resistance tube furnace. The target temperature and holding time were 1473 K (1200 °C) and 2 hours, respectively. In order to simulate the atmosphere condition similar to that of the slab reheating furnace, the N<sub>2</sub>-20pctH<sub>2</sub>O gas mixture was flown by a constant water vapor generator and the dew point analyzer. Using H<sub>2</sub>O instead of simply using O<sub>2</sub> was in particular important to simulate the oxidation mode in the reheating furnace. With and without H in the atmosphere, oxidation modes are different according to Kim and Lee.<sup>[21]</sup> In order to compare the oxidation behavior in the presence of Ni or not, the other sample without the reaction with the NiO-containing flux was also employed for the oxidation experiment.

### C. Analysis

The specimens obtained from the high-temperature reactions (reduction/diffusion and oxidation) were subjected to microscopic analyses. Morphology of the sample, in particular at the interface between the steel and the flux/the oxidized scale was analyzed by a field emission scanning electron microscope (FE-SEM). Concentration profile of Ni after the Ni diffusion, and Cu distribution after the oxidation was analyzed by a field emission electron microprobe analyzer (FE-EPMA) in a wavelength dispersive spectroscopy (WDS) mode and energy dispersive spectroscopy (EDS) mode. For a quantitative analysis for Ni concentration, the Ni peak of WDS

analysis was calibrated using a homemade standard sample (composition in wt pct, Fe-0.09C-0.022~6.34-Ni-1.65Mn-0.31Si-0.30Cu), which was preliminarily prepared in an induction furnace, and analyzed by the ICP.

### D. Pilot-Scale Experiment: Continuous Casting with NiO-Containing Mold Powder

Based on the experimental results, a pilot-scale trial was performed in order to test the proposed idea in a continuously casted steel slab. The test condition for the pilot-scale continuous casting of total 10 ton of the steel were 1.3 m/min casting speed and 140 × 900 mm mold dimension. Starting temperature of the casting in the pilot test was 1544 °C (1817 K). The compositions of steel grade and synthetic mold powder were identical to the previous lab-scale conditions, as shown in Table I. After the pilot casting trials, the slab surface was cut by machining as shown in Figure 3, and the EPMA analysis was conducted for analyzing Ni-enriched behavior.

## III. RESULTS AND DISCUSSIONS

### A. Ni Enrichment by Reduction and Diffusion

Figure 4 shows the WDS elemental mapping result of Ni in the steel sample after high-temperature reduction followed by diffusion. It shows that the diffusion depth of Ni increased with increasing holding time and holding temperature. Ni peak was only detected in the steel matrix, not in the mold flux region. This result shows that the NiO in the mold flux could be easily reduced by alloying elements such as Mn and Si in the steel or Fe.

| Pilot casting conditions |   |
|--------------------------|---|
| Heat (ton / heat)        | 10  |
| Speed (m / min)          | 1.3   |
| Mold Size (mm)           | 140 × 900                                     |
| Steel grade              | MC-steel                                      |
| Mold powder              | CaO/SiO <sub>2</sub> : ~1.1<br>NiO: ~5 wt pct |

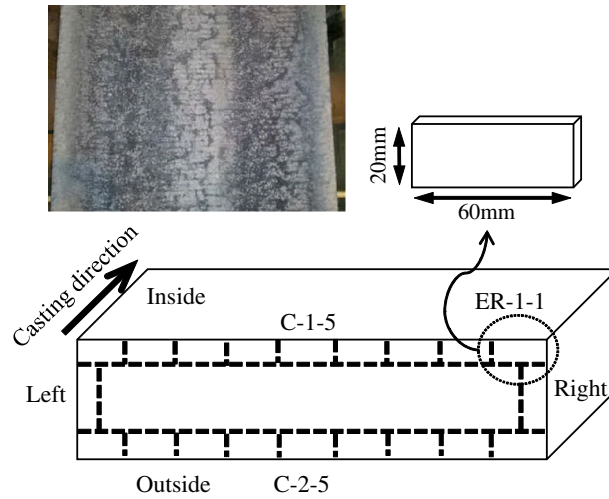


Fig. 3—Pilot caster trial and position of sample cutting for further investigation.

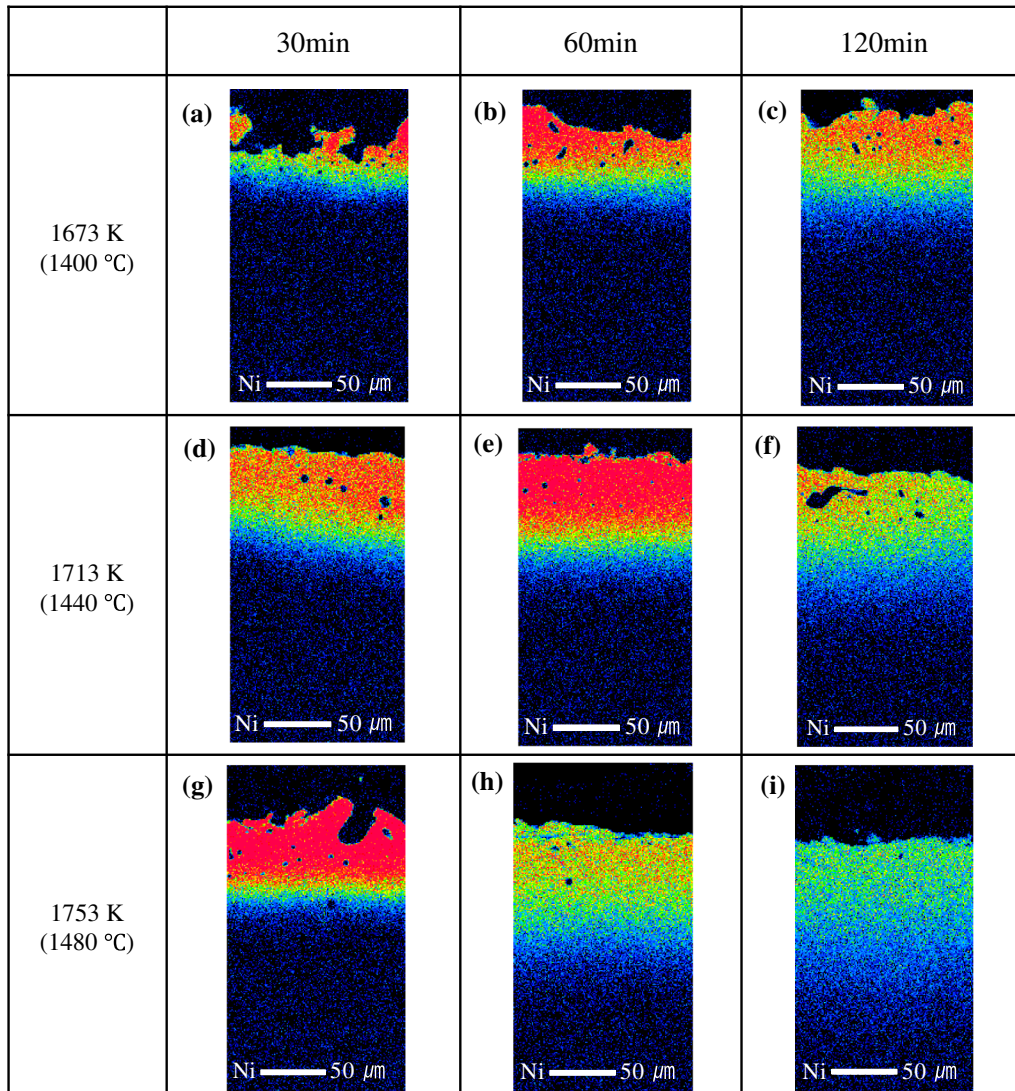


Fig. 4—EPMA mapping result for Ni distribution near steel surface after powder–steel reaction. The color represents concentration of Ni in a semi-quantitative mode, *red* for high concentration and *blue* for low concentration (Color figure online).

As total mass of Ni diffused into the steel matrix could not be evaluated accurately, it was not attempted to confirm the mass balance of Ni between the two phases. However, it is clear that the most NiO in the flux was reduced to provide Ni, and Ni diffused successfully into the steel surface.

Figure 5 shows the WDS quantitative analysis results of the steel samples, heat treated at 1753 K (1480 °C), for the concentration profile of the diffused Ni. Three independent analysis separated each other at 200 μm distance was averaged at each depth from the interface. The analysis was carried out up to 200 μm depth, as seen in the inset photo. The quantitative analysis results are in accordance with the elemental mapping result shown in Figure 4. It is clear that the NiO was reduced into Ni, and the reduced Ni was enriched on the steel surface. It could be a major source of Ni-enriched layer of the steel sample. For 30 minutes heat-treated sample, Ni concentration just near the interface was about 14 wt pct. Ni diffused over 0.05 mm. Increasing the holding time decreased the maximum Ni concentration near the interface, but resulted in longer diffusion depth over 0.1 mm.

Stability of the steel matrix was considered by calculating a phase diagram of the steel system using FactSage FSSkel database.<sup>[22]</sup> The calculated phase diagram is shown in Figure 6. Without the Ni diffusion, the steel samples would have been γ phase at the experimental holding temperatures. Ni diffusion into the steel lowers solidus of the steel, thereby decreasing the stability of γ phase. For example, at 1753 K (1480 °C), the solidus of the steel is about 2 wt pct. Ni. This might have resulted in a partial melting of the sample near the interface during the reduction of NiO. However, according to the observation of the samples, there had not been a formation of liquid phase even at 1753 K (1480 °C). If this had occurred, some portion of metallic droplet would have been observed in the flux side. Therefore, the calculated phase diagram seems to estimate the solidus slightly lower than what it should

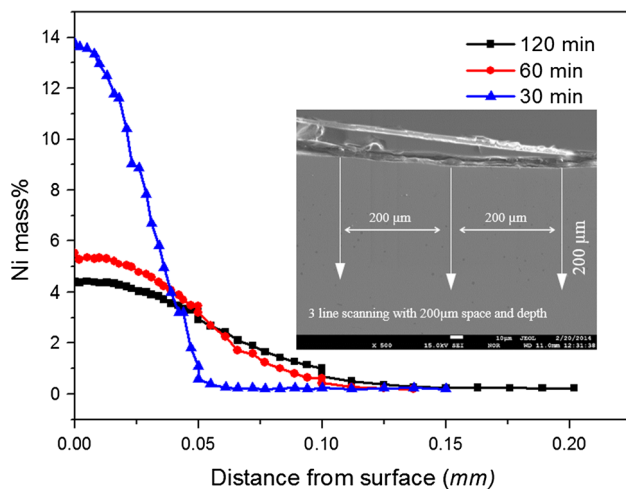


Fig. 5—Quantitative analysis result of Ni distribution into steel surface.

actually be. Nevertheless, the phase diagram tells that Ni diffusion had been occurred in the γ phase.

The diffusion profiles shown in Figure 5 look as if a semi-infinite diffusion of a thin film source for Ni. From the Fick's 2nd law:

$$\frac{\partial C(x, t)}{\partial t} = D \frac{\partial^2 C(x, t)}{\partial x^2}, \quad [1]$$

where  $C(x, t)$  is the Ni concentration at time  $t$  and distance  $x$  from the interface,  $D$  is the diffusivity of Ni in Ni-steel pseudo-binary system as seen in Figure 6. Integrating the above equation yields

$$\ln C(x, t) = \ln \frac{\beta}{\sqrt{\pi D t}} - \frac{x^2}{4 D t}, \quad [2]$$

where  $\beta$  comes from the boundary condition of the Eq. [1], and is related to the total amount of Ni source. Plotting  $\ln C(x, t)$  as a function of  $x^2$  provides

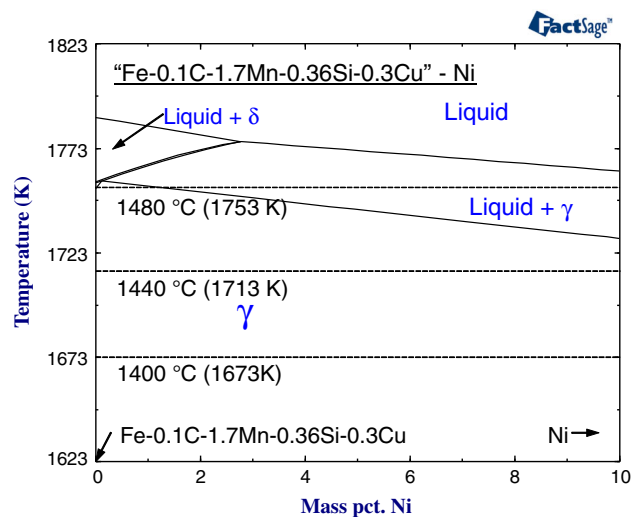


Fig. 6—Calculated phase diagram of the steel system used in the present study.

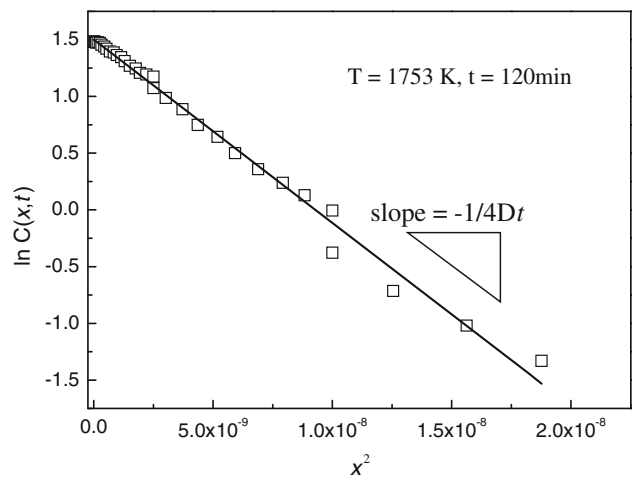


Fig. 7—Determination of diffusivity ( $D$ ) from the measured diffusion profile shown in Fig. 5.

the diffusivity of Ni,  $D$ . According to the Eq. [2]. Figure 7 shows the relation of  $\ln C(x,t)$  vs of  $x^2$  for the sample reacted at 1753 K (1480 °C) for 120 minutes. A good linearity is obtained. From the slope of this plot along with the holding time of 120 minutes, the diffusivity can be obtained. Obtained diffusivity values in a similar manner for the all samples are listed in Table II. All the evaluated diffusivity are in the range of  $1.26$  to  $6.44 \times 10^{-13}$  m<sup>2</sup>/s at temperature between 1673 K (1400 °C) and 1753 K (1480 °C). The obtained values are compared with reported diffusivity of Ni in fcc Fe ( $\gamma$ ) and bcc Fe ( $\alpha$  and  $\delta$ ) in Figure 8.<sup>[23]</sup> Diffusivity obtained in the present study is slightly higher but is in good agreement with the Ni diffusivity in  $\gamma$  phase reported by MacEwan *et al.*,<sup>[23]</sup> extrapolated above  $\gamma/\delta$  transformation temperature of pure Fe. This is consistent with the phase diagram analysis shown in Figure 6 that the Ni diffusion in the present study took place in the  $\gamma$  phase. Although it is not very certain, the higher diffusivity seems to be attributed to the effect of other alloying elements.

From the above observations, it is noted that the formation of Ni-enriched layer is controlled by diffusion of the reduced Ni into the steel. From the diffusivity data shown in Figure 8, it is seen that diffusion of Ni would be much faster in the  $\delta$  phase, not in the  $\gamma$  phase. As the reduction of NiO followed by the diffusion of Ni occurs in a short time in a continuous casting mold and subsequent process before the slab enters into a reheating furnace, it is preferable to have a faster diffusion of

Ni. It suggests that the diffusion would occur more effectively at very initial solidifying temperature where  $\delta$  first appears. Once the NiO is reduced to provide Ni to the steel matrix in the casting mold, the Ni would diffuse first in the  $\delta$  phase, then the steel matrix would transform into  $\gamma$  phase. Once it is known how much NiO is reduced and provide Ni into the steel matrix, probably in the  $\delta$  phase, during the continuous casting condition, it would be possible to predict the concentration profile of Ni during the cooling of the cast slab. This provides Ni distribution near the slab surface before it enters into the reheating furnace. Reduction rate of NiO and/or feeding rate of Ni into the steel matrix is to be further investigated.

### B. High-Temperature Oxidation of the Steel with Ni-Enriched Layer at the Surface

In order to verify the expected decrease of Cu hot shortness during a high-temperature oxidation according to the proposed idea, the Ni-layered sample A which was obtained after the previous experiment (Sections II-B and III-A) was used. For the sample A, depth of Ni diffusion was approximately 100–150  $\mu$ m from the surface as shown in Figure 5. In order to compare the oxidation behavior in a sample with no Ni as described in Section II-C, a sample which was taken from the slab but had not been reacted with the NiO-containing flux B was also employed. The high-temperature oxidation was carried out at 1673 K

Table II. Calculation Result of Diffusivity for Ni into Steel

| Temperature [K (°C)] | NiO (Weight Percent) | Time (s) | $-1/4Dt$            | $D$ (m <sup>2</sup> /s) |
|----------------------|----------------------|----------|---------------------|-------------------------|
| 1753 (1480)          | 5                    | 1800     | $-1.10 \times 10^9$ | $1.26 \times 10^{-13}$  |
|                      |                      | 3600     | $-2.31 \times 10^8$ | $3.01 \times 10^{-13}$  |
|                      |                      | 7200     | $-1.61 \times 10^8$ | $2.15 \times 10^{-13}$  |
| 1713 (1440)          | 5                    | 1800     | $-2.16 \times 10^8$ | $6.44 \times 10^{-13}$  |
|                      |                      | 3600     | $-3.68 \times 10^8$ | $1.89 \times 10^{-13}$  |
|                      |                      | 7200     | $-1.06 \times 10^8$ | $3.29 \times 10^{-13}$  |
| 1673 (1400)          | 5                    | 3600     | $-1.55 \times 10^8$ | $4.47 \times 10^{-13}$  |
|                      |                      | 7200     | $-2.79 \times 10^8$ | $1.24 \times 10^{-13}$  |

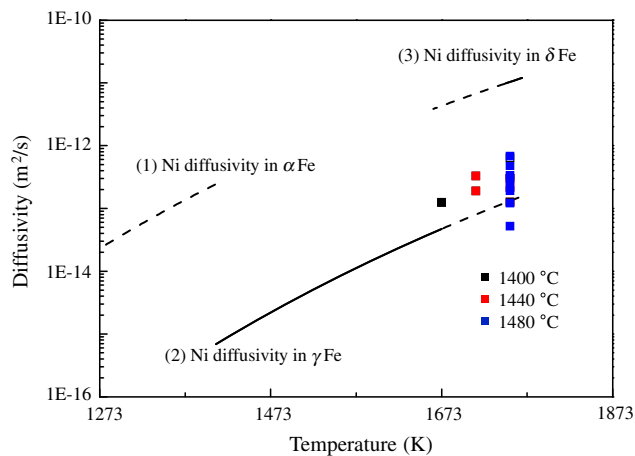


Fig. 8—Comparison of measured diffusivity and reference data.<sup>[23]</sup>

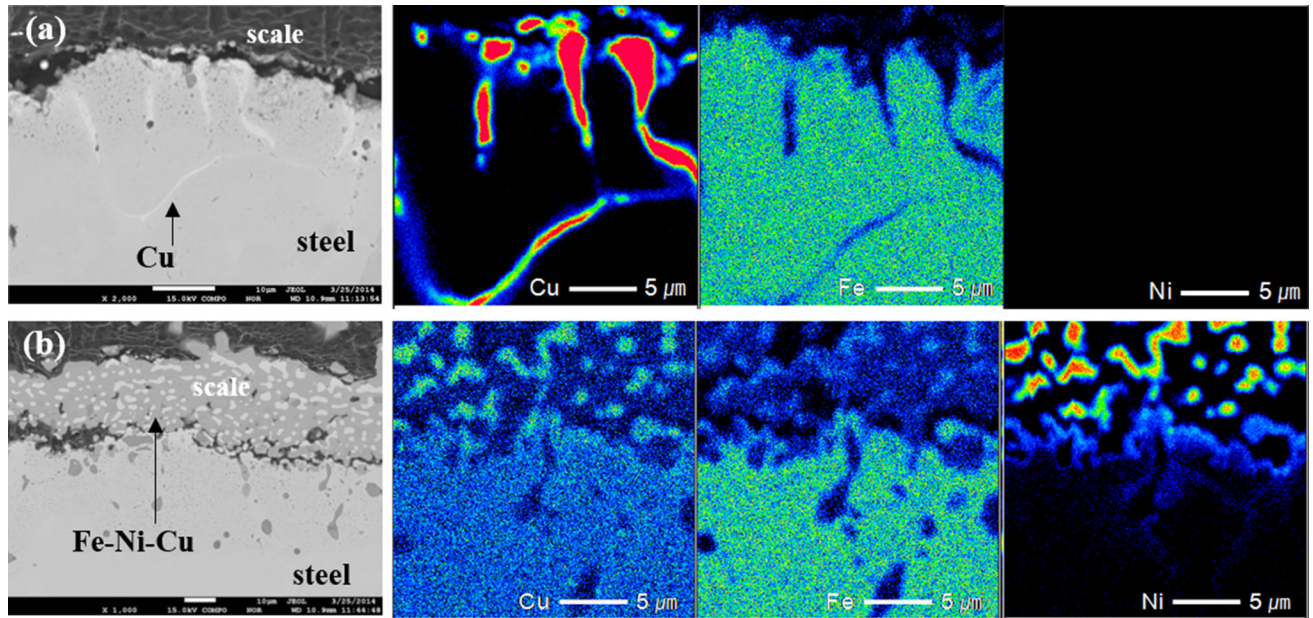


Fig. 9—SEM and EPMA results after high-temperature oxidation, (a) without nickel rich layer on steel surface (W/O Ni sample), (b) with nickel rich layer on steel surface (W/Ni sample).

(1200 °C) for 2 hours under  $N_2$ -20pct $H_2O$  atmosphere. This is because LNG combustion gas is usually supplied as a fuel gas in the commercial reheating furnace, and this generates  $H_2O$ . It is known that the oxidation behavior of steel under  $O_2$  and  $H_2O$  are very different.<sup>[24–29]</sup>

Figure 9 shows the results of high-temperature oxidation of two samples. Back-scattered images are shown for the sample A and B, respectively. Figure 9(a) shows result of the sample A after the oxidation. It shows that Cu-rich phase is clearly seen near the surface of the steel. Infiltrated Cu, probably along the grain boundary is also seen. Enriched Cu was hardly observed in the scale side. However, as seen in Figure 9(b), the oxidation of the sample B resulted in less accumulation of Cu-enriched phase near the surface of the steel matrix. On the other hand, the Cu-enriched phase was located in the scale. No infiltrated Cu-rich phase was observed, contrary to the sample A. The diffused Ni was accumulated in the Cu-rich phase in the scale. The infiltrated Cu-rich phase in the sample A (Figure 9(a)) and the occluded Cu/Ni-enriched phase was further analyzed by FE-SEM and EDS. Concentrations of these samples were projected onto Fe-Ni-Cu ternary isothermal section at 1673 K (1200 °C), shown in Figure 10, calculated by FactSage FSSkel database.<sup>[22]</sup> While the composition of the infiltrated Cu-rich phases of the sample A fall mostly in liquid or liquid +  $\gamma$  two-phase region, that of the occluded Cu/Ni-enriched phases of the sample B is in a  $\gamma$  single-phase region. This observation is in consistent with Imai *et al.*<sup>[16]</sup> Oxidation of steel increases local Cu concentration near the surface of the steel, and causes a precipitation of Cu-rich phase in the absence of Ni as was for the sample A (Figure 9). In particular, this is a liquid phase at 1673 K (1200 °C). On the other hand, in the case of the sample B, not only Cu but also Ni were simultaneously enriched. This resulted in the increase of

Cu and Ni contents, but leaves the phase still in the  $\gamma$  single-phase region due to the increase of Cu solubility by Ni.<sup>[30]</sup>

### C. Development of Ni-Enriched Layer in a Continuously Cast Slab: Pilot-Scale Trial with NiO-Containing Flux

In order to evaluate whether the proposed idea could be realized in a commercial continuous casting condition, a pilot-scale trial was carried out as described in Section II–D. The casting condition and cast slab are shown in Figure 3. Figure 11 shows the results of EPMA elemental mapping for Ni on an edge side of the wide face. Ni-enriched depth, defined as the concentration over 0.022 wt pct Ni which was contained in steel as a tramp element from scrap, was evaluated over the wide face. As seen in the figure, the depth and the Ni concentration in the Ni-enriched layer were very uneven. The depth varied from a few hundreds  $\mu m$  to over 2 mm. Comparing the Ni diffusion profiles measured in the lab-scale test discussed in the Section III–A, the observed Ni depth profile in the cast slab is much longer. It is considered that most reduction of NiO in the flux and absorption into the steel were occurred at very early stage of solidification where  $\delta$  phase is stable. Under the pilot casting conditions, duration of the  $\delta$  phase is estimated to be less than 0.5 second at the casting speed of 1.3 m/min. During such a short time, the diffusion depth would only be less than 50  $\mu m$  by simple finite differential calculation with interdiffusion coefficient of Ni into Fe.<sup>[23]</sup> Once the  $\delta$  phase transforms into  $\gamma$  phase, the Ni diffusion would be much slower. Thus, expected Ni diffusion depth would not be in the range of 1 to 2 mm, contrary to the observation made in the cast slab. In the present study, the pilot-scale casting showed that some part of the slab had very thick Ni-enriched layer. This fact implies that there might have been accelerated

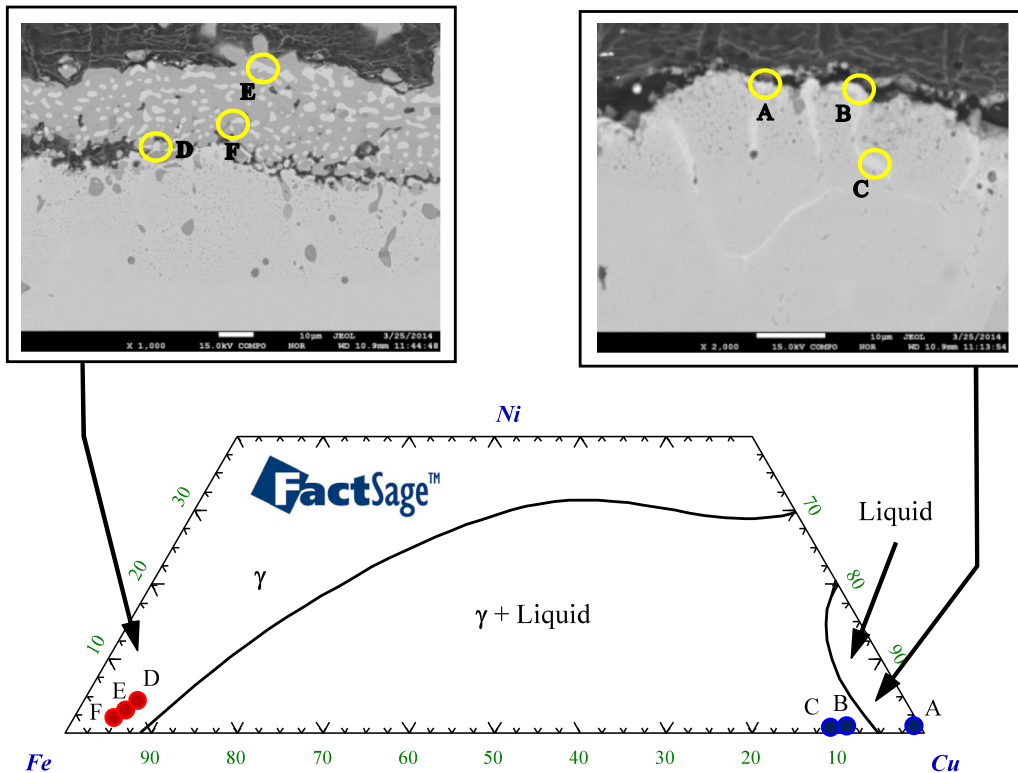


Fig. 10—Fe-Ni-Cu phase diagram at 1473 K.

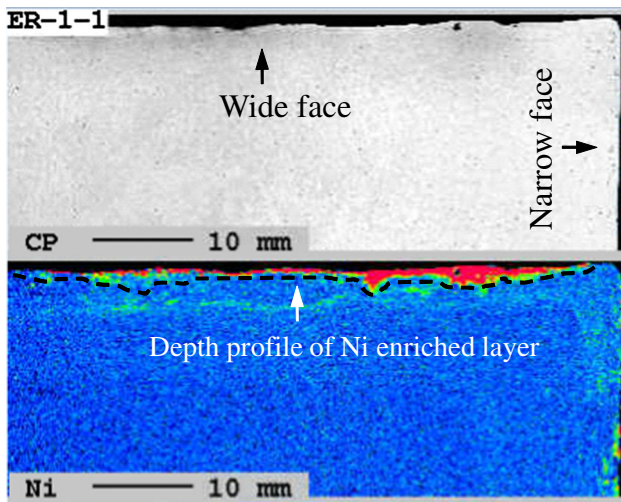


Fig. 11—Result of FE-EPMA examinations and nickel-enriched depth profile.

diffusion involving liquid phase, as enrichment of Ni lowers the solidus of the steel as seen in Figure 6. Some other factors may be thought as complicated initial solidification, turbulence mixing between liquid mold flux and solidifying shell, *etc.*

This also suggests the possibility that the Ni-enriched layer was developed not only by the reduction/diffusion route, but also by an additional mechanism which requires further investigation. Overall, this would help to prevent from Cu enrichment of the steel during

oxidation in the reheating furnace. During the oxidation of steel, Fe is depleted by forming oxide scale. At the same time, Cu is enriched at the interface between the steel and the scale. In order to prevent the Cu enrichment effectively, the Ni-enriched layer should be remained or react with the enriched Cu near the interface during further oxidation. Webler *et al.*<sup>[18]</sup> investigated the effect of the presence of Cu and Ni, respectively, on the oxidation rate. They showed that the presence of Cu did not influence the total amount of oxide formed, compared to that of Cu-free iron. On the other hand, the presence of Ni reduced the total amount of oxide formed. Oxidation rate was also lowered as half as the oxidation rate in the Ni-free iron. Therefore, in order to investigate the effective Ni-enriched layer in order to prevent Cu enrichment, the effect of Ni on the oxidation rate should be taken into account. According to Abuluwefa *et al.*,<sup>[31,32]</sup> an oxidation of commercial low-carbon steel which has small amount of Cu and Ni (Fe-0.04C-0.2Mn-0.02Si-0.05Cu-0.03Ni, in wt pct.) in the industrial walking-beam steel reheating furnace, the scale grows following the parabolic rate law. From the obtained rate constant, the weight of oxidized scale at 1423 K (1150 °C) for 120 minutes could be calculated as 0.1 g/cm<sup>2</sup>. Assuming the scale is wüstite, the depleted steel depth could be calculated as 107.96 μm for the 120 minutes. According to the present research shown in Figure 5, Ni should be enriched more than 110 μm depth during 120 minutes. In the pilot-scale trial, there was also enough enriched Ni layer as can be seen in Figure 11. Therefore, it is thought that use of the



NiO-containing flux is promising to suppress the Cu enrichment in the steel slab effectively, during oxidation in the reheating furnace. Nevertheless, further investigations are required to understand the exact mechanism of Ni absorption into the steel matrix, and absorption rate of the Ni. The latter can be useful in the prediction of Ni-enriched layer profile during continuous casting and subsequent processing of the steel slab.

#### IV. CONCLUSIONS

A novel idea has been proposed and examined for preventing Cu enrichment in the continuously cast steel slab, which usually occurs when scrap-based steel slab is reheated before rolling process. A series of lab-scale and pilot-plant-scale experiments were carried out, and the following results were obtained:

- (1) Ni containing mold powder was easily reduced at initial solidification temperature and formed Ni-enriched layer near the steel surface by the lab-scale experiment. Obtained diffusivity of Ni in the steel was in good agreement with the extrapolated diffusivity of Ni in  $\gamma$ -Fe at the temperature where the  $\gamma$ -Fe is not stable.
- (2) The Ni-enriched steel sample was further subjected to the oxidation at 1673 K (1200 °C) under the  $N_2$ -20% $H_2O$  gas mixture. Compared with the other sample without Ni-enriched layer, the Ni-enriched steel sample was relatively inert to the Cu enrichment. The microscopic observation at the interface between the steel and the scale were in agreement with the previous investigations regarding the role of Ni for the prevention of Cu hot shortness.<sup>[16–19]</sup>
- (3) From the pilot-scale casting results, the Ni enrichment was irregularly developed. Depth of the Ni-enriched layer was longer than what was obtained in the lab-scale experiment. Results suggested an additional mechanism of Ni enrichment other than reduction of NiO followed by diffusion of Ni. It requires further investigation.

#### REFERENCES

1. C. Ryman and M. Larsson: *ISIJ Int.*, 2006, vol. 46, pp. 1752–58.
2. D. Young: *High Temperature Oxidation and Corrosion of Metals*, Elsevier, 2008, pp. 185–193.
3. T. Kajitani, M. Wakoh, S. Ogibayashi, and S. Mizoguchi: *Tetsu-to-Hagané*, 1995, vol. 81, pp. 185–90.
4. H.G. Katayama, T. Momono, M. Doe, and H. Saitoh: *ISIJ Int.*, 1994, vol. 34, pp. 171–76.
5. A. Hartman, C. Williamson, and D. Davis: *Iron Steelmaker*, 1996, vol. 23, pp. 43–45.
6. K. Matsumaru, M. Susa, and K. Nagata: *Tetsu-to-Hagané*, 1996, vol. 82, pp. 799–804.
7. M. Sasabe, E. Harada, and S. Yamashita: *Tetsu-to-Hagané*, 1996, vol. 82, pp. 129–34.
8. R.E. Brown, H.V. Divilio, and R.J. Divilio: *Removal of Copper, Tin and other Impurities from Iron Scrap*. BuMines, RI, 1975, pp. 1–31.
9. C. Wang, T. Nagasaka, and M. Hino: *ISIJ Int.*, 1991, vol. 31, pp. 1300–08.
10. C. Wang, T. Nagasaka, and M. Hino: *ISIJ Int.*, 1991, vol. 31, pp. 1309–15.
11. X. Chen, N. Ito, and K. Nakashima: *Tetsu-to-Hagané*, 1995, vol. 81, pp. 959–64.
12. R.D. Morales and N. Sano: *Ironmaking and Steelmaking*, 1982, vol. 9, pp. 65–76.
13. T. Hidani, K. Takemura, and R.O. Suzuki: *Tetsu-to-Hagané*, 1996, vol. 82, pp. 135–40.
14. T. Maruyama, H.G. Katayama, and T. Momono: *Tetsu-to-Hagané*, 1998, vol. 84, pp. 243–48.
15. H. Ono-Nakazato, K. Taguchi, Y. Seike, and T. Usui: *ISIJ Int.*, 2003, vol. 43, pp. 1691–97.
16. N. Imai, N. Komatsubara, and K. Kunishige: *ISIJ Int.*, 1997, vol. 37, pp. 224–31.
17. M. Hatano and K. Kunishige: *Tetsu-to-Hagané*, 2003, vol. 89, pp. 42–49.
18. B. Webler, L. Yin, and S. Sridhar: *Metall. Mater. Trans. B*, 2008, vol. 39B, pp. 725–37.
19. L. Yin, S. Balaji, and S. Sridhar: *Metall. Mater. Trans. B*, 2010, vol. 41B, pp. 598–611.
20. A. Takemura, K. Kunishige, S. Okaguchi, and K. Fujiwara: *Tetsu-to-Hagané*, 2009, vol. 95, pp. 369–77.
21. S.-W. Kim and H.-G. Lee: *Steel Res. Int.*, 2009, vol. 80, pp. 121–29.
22. C.W. Bale, E. Belisle, P. Chartrand, S.A. Decterov, G. Eriksson, K. Hack, I.-H. Jung, Y.-B. Kang, J. Melancon, A.D. Pelton, C. Robelin, and S. Petersen: *Calphad*, 2009, vol. 33, pp. 295–311.
23. E.A. Brandes and G.B. Brook: *Smithells Metals Reference Book*, The Bath Press, London, 1992, p. 13.
24. C.W. Tuck, M. Odgers, and K. Sachs: *Corros. Sci.*, 1969, vol. 9, pp. 271–85.
25. K. Honda: *Oxid. Met.*, 1992, vol. 38, pp. 347–63.
26. N. Birks: *Electrochem. Soc. Proc. Symp.*, 1976, vol. 1, pp. 215–60.
27. P. Kofstad: *High Temperature Corrosion*, Elsevier, London, 1988, pp. 120–25.
28. Y. Kondo: *ISIJ Int.*, 2007, vol. 47, pp. 1309–14.
29. R.Y. Chen and W.Y.D. Yuen: *Oxid. Met.*, 2003, vol. 59, pp. 433–68.
30. H. Ohtani, H. Suda, and K. Ishida: *ISIJ Int.*, 1997, vol. 37, pp. 207–16.
31. H.T. Abuluwefa, R.I.L. Guthrie, and F. Ajersch: *Metall. Mater. Trans. A*, 1997, vol. 28A, pp. 1633–42.
32. H.T. Abuluwefa, R.I.L. Guthrie, and F. Ajersch: *Metall. Mater. Trans. A*, 1997, vol. 28A, pp. 1643–51.